CHEMISTRY
A EUROPEAN JOURNAL

DOI: 10.1002/chem.200600955

Structures of the High-Temperature Solid Phases of the Odd-Numbered Fatty Acids from Tridecanoic Acid to Tricosanoic Acid

Gabin Gbabode,*[a] Philippe Negrier,[a] Denise Mondieig,[a] Evelyn Moreno Calvo,[b] Teresa Calvet,[b] and Miquel Àngel Cuevas-Diarte[b]

Abstract: Crystal structures of the high-temperature phases of odd-numbered fatty acids ($C_nH_{2n-1}OOH$) from tridecanoic acid ($C_{13}H_{25}OOH$) to tricosanoic acid ($C_{23}H_{45}OOH$) are presented in this article. They have been determined from high-quality X-ray powder-diffraction patterns. Two types of high-temperature phases are adopted: one monoclinic $A2/a$ with $Z=8$ for the fatty acids with $n=13$ and $n=15$, denoted as C″, and one monoclinic $P2_1/a$ with $Z=4$ for the longer-chain fatty acids, denoted as C′. It appears that the packing arrangement of the alkyl chains and of the carboxyl groups is similar in all of the structures. However, the arrangement at the methyl-group interface differs between the C′ and C″ forms. A survey of the intermolecular interactions involved in these polymorphs coupled with a study of the effects of temperature on the structures have led us to a better understanding of the arrangement of the molecules within the high-temperature solid phases of odd-numbered fatty acids.

Keywords: bilayers · hydrogen bonds · polymorphism · thermal motion · van der Waals interactions

Introduction

Higher fatty acids of the formula $C_nH_{2n-1}OOH$ are composed of long, saturated aliphatic chains with a carboxyl group at one of their extremities. It is well known that long-chain aliphatic compounds adopt several solid forms, with different configurations of the packing of the molecules in and between the layers.[1–5] Typically, the A′, B′, C′, C″, and D′ forms[6–9] are adopted by the saturated fatty acids with an odd number of carbon atoms, whereas the A, B, C, and E forms[6–10] are adopted by those with an even number of carbon atoms. All of these fatty acids exhibit at least one solid–solid transition prior to melting,[7–9] and we usually distinguish the high-temperature phase that is stable just below the melting point from the low-temperature phase observable at lower temperatures. For odd-numbered fatty acids, the high-temperature phase may be the C′ or the C″ form.[6] For years, only the structure of the C′ form of hendecanoic acid ($C_{11}H_{21}OOH$) had been reported,[11] and, moreover, it had not been fully resolved (two-dimensional (2D) structure). Recently, Bond solved the crystal structures of the high-temperature solid phases of all fatty acids from hexanoic acid ($C_6H_{11}OOH$) to pentadecanoic acid ($C_{15}H_{29}OOH$) from single crystals.[6] The results obtained for the odd-numbered fatty acids showed that, just below their respective melting points, the fatty acids with chain length from $n=7$ to $n=11$ adopt the C′ form, whereas tridecanoic acid and pentadecanoic acid adopt the C″ form.

In the present article, we focus on longer-chain odd-numbered fatty acids, specifically those with 13 to 23 carbon atoms. These compounds have high enthalpies of melting and they are also thermo-adjustable by means of their chain length. These fatty acids, as well as their mixed samples, could therefore be potential candidates for applications in the field of energy storage or thermal protection, as has been demonstrated for alkanes[12,13] and alkanols.[14,15] In this context, it is important to know the crystal structures of the high-temperature solid phases, as it is these that are involved in the melting process.

Crystal structure determination of the high-temperature phases of odd-numbered fatty acids is not an easy task. These solid forms are only stable in a narrow temperature range just below the melting point, and this temperature interval becomes narrower with increasing chain length.[16,17]

[a] Dr. G. Gbabode, Dr. P. Negrier, Dr. D. Mondieig
CPMOH, Université Bordeaux I
Alliages Moléculaires et Stockage d'Énergie
351, cours de la Libération, 33405 Talence Cedex (France)
Fax: (+33) 5 40 00 66 86
E-mail: gabin_g@yahoo.fr

[b] E. Moreno Calvo, Prof. T. Calvet, Prof. M. À. Cuevas-Diarte
Departament Cristallografia, Mineralogia i Dipòsits Minerals
Facultat de Geologia, Universitat de Barcelona
Martí y Franqués, s/n, 08028 Barcelona (Spain)

The growth of single crystals is therefore very complicated, and the degree of difficulty goes on increasing for the longer acids. Some attempts have been made to grow such crystals, but without success. As a consequence, we have now determined their crystal structures from X-ray powder-diffraction patterns measured at the appropriate temperatures. The module POWDER SOLVE[18] of the MATERIAL STUDIO application[19] has been used to resolve the crystal structures.

In the first part of this paper, the polymorphism of the fatty acids from $C_{13}H_{25}OOH$ to $C_{23}H_{45}OOH$ is briefly described. Data from both calorimetric and X-ray powder-diffraction measurements are presented. A detailed analysis of the X-ray powder-diffraction patterns of the high-temperature solid forms is then described. Their crystal structures are presented and the packing arrangement of the molecules throughout the studied series is discussed. In particular, the results obtained for tridecanoic acid and pentadecanoic acid are compared with those obtained by Bond. Finally, the effects of temperature are analysed and related to the packing arrangement of the molecules.

Results

Calorimetric analysis: The DSC traces obtained for the six fatty acids were, in each case, indicative of the occurrence of a solid–solid transition before melting (Figure 1). The temperature interval between the two transitions diminishes with increasing chain length (at least up to $C_{19}H_{37}OOH$; this temperature interval is a little wider for $C_{21}H_{41}OOH$ and $C_{23}H_{45}OOH$ than for $C_{19}H_{37}OOH$).

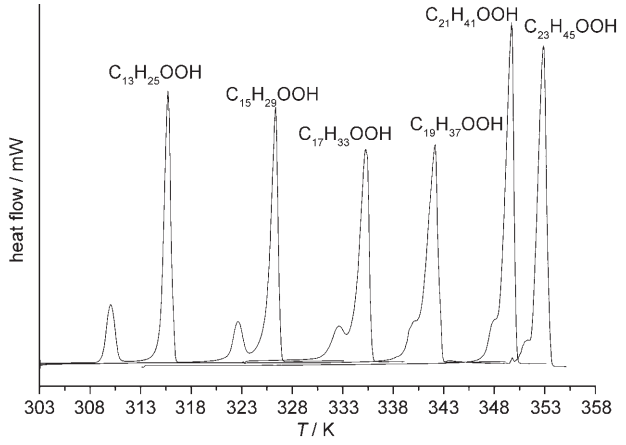

Figure 1. Extract of the DSC signals obtained with a heating rate of 2 K min^{-1}.

The various transitions observed for these materials have been characterised by both X-ray diffraction and thermal analysis. The measured temperatures, entropies, and enthalpies are displayed in Table 1. As mentioned in the literature,[7–9] $C_{13}H_{25}OOH$ adopts the A′ form at room temperature. A low-energy reversible transition was observed at 287.7 K, which we attribute to an A'_l (l for low)→A'_h (h for high) transition. Such a transition has been previously observed by Kaneko et al.[20] for pentadecanoic acid. All of the other acids adopt the B′ form at room temperature, as predicted by many authors.[8,9] However, we have also observed A'_l and A'_h solid phases for samples of $C_{15}H_{29}OOH$. The temperature of the A'_h→C″ transition is lower than that of the B′→C″ transition (Table 1). Therefore, B′ is more stable than A′ in the vicinity of the transition point for pentadecanoic acid. Irrespective of the low-temperature phases, the high-temperature phases are the C″ form for $C_{13}H_{25}OOH$ and $C_{15}H_{29}OOH$ and the C′ form for the four other acids.

The evolution of the solid–solid transition temperatures and the melting points shown in Figure 2 is in agreement with the work of von Sydow and Stenhagen,[16] in which these parameters were plotted for the odd-numbered acids from $n=13$ to $n=29$.

The enthalpies and entropies of melting increase almost linearly with increasing chain length. These trends reflect the regular incremental lengthening of the hydrocarbon chain by the addition of two CH_2 groups on going from one acid to the next.

Indexing of the X-ray powder-diffraction patterns: Taking into account the temperatures of the transitions determined by thermal analysis, X-ray powder-diffraction patterns of the high-temperature phases were recorded at 313.0, 324.0, 333.0, 340.0, 346.4, and 351.7 K for $C_{13}H_{25}OOH$, $C_{15}H_{29}OOH$, $C_{17}H_{33}OOH$, $C_{19}H_{37}OOH$, $C_{21}H_{41}OOH$, and $C_{23}H_{45}OOH$, respectively. All of the reflections of the powder patterns of $C_{13}H_{25}OOH$ and $C_{15}H_{29}OOH$ have been indexed to the C″ form, which is monoclinic with space group $A2/a$ and has eight molecules in the unit cell. For the fatty acids from $C_{17}H_{33}OOH$ to $C_{23}H_{45}OOH$, the reflections have been indexed to the C′ form, which is also monoclinic, but has space group $P2_1/a$ and $Z=4$. The measured and cal-

Table 1. Temperatures (T in K), enthalpies (ΔH in kJ mol^{-1}), and entropies (ΔS in J mol^{-1} K^{-1}) of the various phase transitions.

	Solid–solid transition (S_{III}→S_{II})				Solid–solid transition (S_{II}→S_I)				Melting (S_I→liquid)			
	S_{III}	T	ΔH	ΔS	S_{II}	T	ΔH	ΔS	S_I	T	ΔH	ΔS
$C_{13}H_{25}OOH$	A'_l	287.7(6)	0.06(1)	0.21(4)	A'_h	309.1(4)	8.5(3)	27(1)	C″	314.6(5)	33(1)	105(3)
$C_{15}H_{29}OOH$	A'_l	295.5(5)	0.27(7)	0.9(2)	A'_h	320.8(3)	–	–	C″	325.5(4)	40.4(6)	124(2)
$C_{15}H_{29}OOH$	–	–	–	–	B′	321.9(4)	8.2(6)	25(2)	C″	325.5(4)	40.4(6)	124(2)
$C_{17}H_{33}OOH$	–	–	–	–	B′	331.2(5)	7.5(9)	23(3)	C′	333.5(5)	46.5(9)	139(3)
$C_{19}H_{37}OOH$	–	–	–	–	B′	339.0(4)	7.4(6)	22(1)	C′	340.4(3)	57(1)	167(3)
$C_{21}H_{41}OOH$	–	–	–	–	B′	344.6(4)	5(1)	13(3)	C′	346.7(5)	63(3)	183(9)
$C_{23}H_{45}OOH$	–	–	–	–	B′	349.9(4)	2.5(6)	7(2)	C′	352.0(5)	75(3)	212(9)

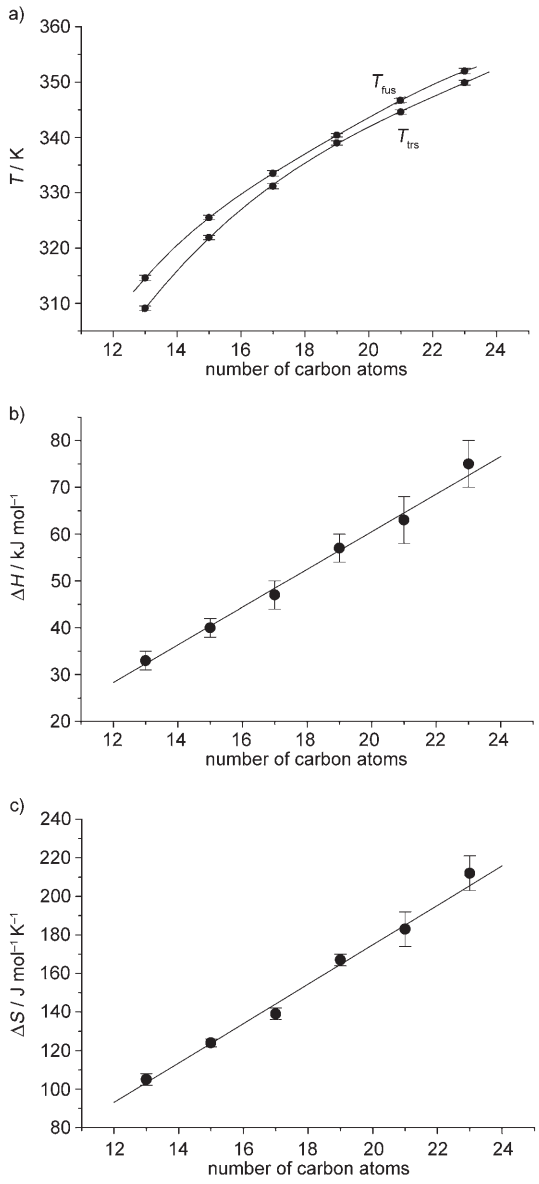

Figure 2. Evolution of some thermodynamic quantities with increasing chain length: a) temperatures of solid–solid transition (T_{trs}) and of melting (T_{fus}), b) enthalpies of melting, and c) entropies of melting.

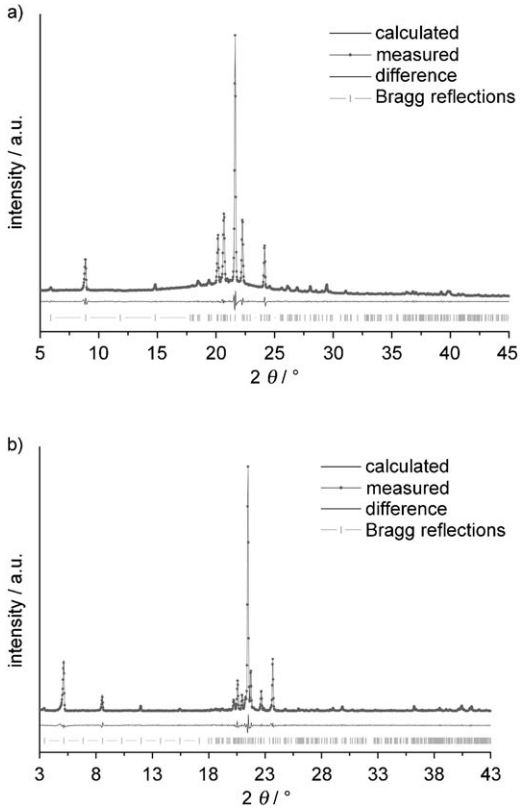

Figure 3. Superimposition of the experimental and calculated X-ray powder-diffraction patterns (Pawley refinement) obtained for a) $C_{13}H_{25}OOH$ and b) $C_{23}H_{45}OOH$.

culated powder patterns (Pawley refinement[21]) of $C_{13}H_{25}OOH$ and $C_{23}H_{45}OOH$ are shown superimposed in Figure 3.

For the fatty acids from $C_{17}H_{33}OOH$ to $C_{23}H_{45}OOH$, the hypothetical cell parameters of the $A2/a$ C″ forms have also been calculated by analogy with the cell parameters of $C_{13}H_{25}OOH$ and $C_{15}H_{29}OOH$ by using the Win_CELREF and Win_CRISDR programs.[22] Figure 4 shows the Pawley fits for $C_{17}H_{33}OOH$ and $C_{19}H_{37}OOH$ obtained for the $P2_1/a$ and $A2/a$ arrangements in the 2θ domain (25–32°), which exhibits the most marked differences between the two arrangements for each compound. Trial assignments of the $A2/a$ phase for the fatty acids from $C_{17}H_{33}OOH$ to $C_{23}H_{45}OOH$ invariably gave worse agreement of the experimental and calculated X-ray diffraction patterns. As an example, the relatively strong reflection at around 29° is never taken into account in the $A2/a$ lattice, whereas it corresponds to the $\bar{2}11$ reflection in the $P2_1/a$ lattice for the four fatty acids. All reflections are indexed with the $P2_1/a$ lattice of the C′ form for the fatty acids from $C_{19}H_{37}OOH$ to $C_{23}H_{45}OOH$, whereas this is not quite the case for $C_{17}H_{33}OOH$. Indeed, it is evident from Figure 4a that the weak reflection at 29.5° is not possible with the $P2_1/a$ lattice, whereas it is with the $A2/a$ lattice. It may be assumed that this sample also contains a small amount of the C″ form, as this fatty acid is at the limit between the occurrence of the C′ and C″ forms in the series.

The cell parameters, the space groups, and the calculated densities determined for the high-temperature solid forms of the six fatty acids are displayed in Table 2. The agreement factor, *Rwp*, obtained after Pawley refinement, is also given for each acid. In addition, the crystallographic data determined by von Sydow[11] for the C′ form of $C_{11}H_{21}OOH$ and by Bond[6] for the C′ form of $C_{11}H_{21}OOH$ and the C″ forms of $C_{13}H_{25}OOH$ and $C_{15}H_{29}OOH$ are also included.

The cell parameters determined for $C_{13}H_{25}OOH$ and $C_{15}H_{29}OOH$ are in good agreement with those obtained by Bond. The *a* parameter decreases as the number of carbon

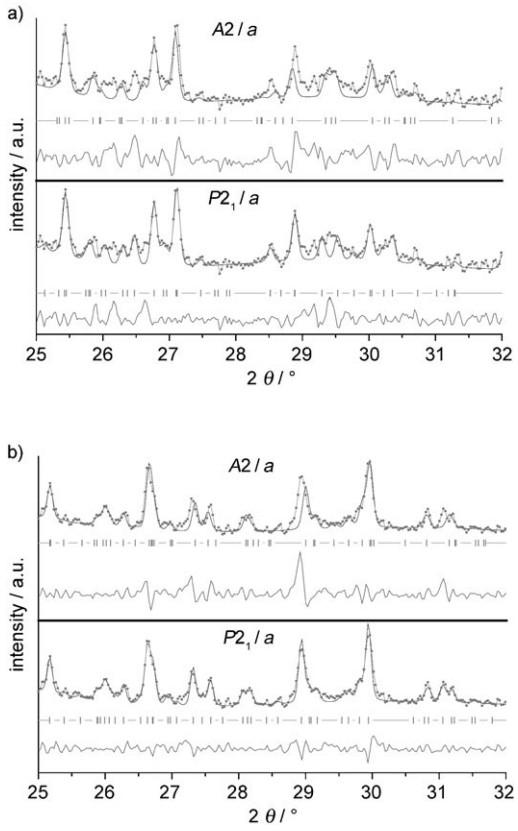

Figure 4. Superimposition in the 25–32° 2θ domain of the Pawley fits obtained using the $P2_1/a$ and $A2/a$ lattices for a) $C_{17}H_{33}OOH$ and b) $C_{19}H_{37}OOH$.

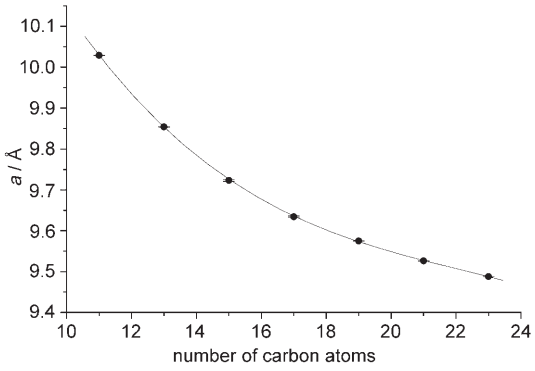

Figure 5. Evolution of the a parameter with increasing chain length from $C_{11}H_{21}OOH$ to $C_{23}H_{45}OOH$.

Table 2. Crystallographic data determined for the high-temperature solid forms of the odd-numbered fatty acids from $C_{13}H_{25}OOH$ to $C_{23}H_{45}OOH$, together with those found in the literature. The non-standard space groups settings $A2/a$ and $P2_1/a$ have been chosen for convenience, so that the chain axis is almost parallel to the c axis.

	Ref.	T [K]	Rwp	Density [g cm^{-3}]	Space group	Z	a [Å]	b [Å]	c [Å]	β [°]
$C_{11}H_{21}OOH$	[11]	296	–	–	$P2_1/a$	4	9.62(3)	4.92(1)	34.2(1)	131.3(3)
	[6]	300	–	0.984	$P2_1/a$	4	10.029(1)	4.912(1)	35.10(1)	133.36(1)
$C_{13}H_{25}OOH$	this work	313	0.031	0.981(1)	$A2/a$	8	9.854(1)	4.940(1)	73.66(1)	125.95(1)
	[6]	310	–	0.983	$A2/a$	8	9.812(1)	4.943(1)	73.74(1)	125.88(1)
$C_{15}H_{29}OOH$	this work	324	0.033	0.975(1)	$A2/a$	8	9.724(2)	4.952(1)	84.02(3)	125.30(1)
	[6]	320	–	0.975	$A2/a$	8	9.720(1)	4.956(1)	84.02(1)	125.29(1)
$C_{17}H_{33}OOH$	this work	333	0.034	0.974(1)	$P2_1/a$	4	9.634(2)	4.953(1)	50.03(1)	129.44(1)
$C_{19}H_{37}OOH$	this work	340	0.035	0.974(1)	$P2_1/a$	4	9.575(1)	4.953(1)	54.99(1)	128.72(1)
$C_{21}H_{41}OOH$	this work	346.4	0.035	0.970(1)	$P2_1/a$	4	9.526(1)	4.957(1)	60.18(1)	128.10(1)
$C_{23}H_{45}OOH$	this work	351.7	0.029	0.969(1)	$P2_1/a$	4	9.488(1)	4.957(1)	65.23(1)	127.63(1)

atoms increases, following a regular curve (Figure 5) from $C_{11}H_{21}OOH$ to $C_{23}H_{45}OOH$. Furthermore, the b parameter is nearly constant for all of these acids.

The density decreases with increasing chain length. Indeed, the temperature of acquisition increases with increasing chain length and so does the thermal motion, which tends to increase the volume of the crystal lattice. The densities calculated for the high-temperature phases are all around 0.99 g cm^{-3}, whereas they are a little higher, around 1.02 g cm^{-3}, for the low-temperature phases.[23,24]

As a conclusion of the two previous sections, it can be stated that the evolution with increasing chain length of several measured quantities (transition temperature, enthalpy, a parameter) are described by continuous curves from $C_{13}H_{25}OOH$ to $C_{23}H_{45}OOH$, irrespective of the high-temperature solid phase that is adopted (C″ for $C_{13}H_{25}OOH$ and $C_{15}H_{29}OOH$; C′ for the longer acids).

Crystal structures of the high-temperature phases: The crystal structures determined for the six fatty acids correspond to the best compromise between Rietveld refinement and energy minimisation (see the Experimental Section for more details). Projections in the (a,c) plane of the crystal structures of the C″ form of $C_{15}H_{29}OOH$ and of the C′ form of $C_{21}H_{41}OOH$ are presented in Figure 6. The molecules are stacked in bilayers in both forms, with dimers being formed by hydrogen bonding between the carboxyl groups. The crystal structures show alternating methyl- and carboxyl-group interfaces along the c axis, as is visible in Figure 6. The $A2/a$ structure is a twofold version of the $P2_1/a$ structure. The two types of structures are centrosymmetric and the hydrogen bonds bridge the carboxyl groups of molecules related by inversion centres. In these representations, it can be seen that the molecules are not situated in the same positions in the $A2/a$ lattice and the $P2_1/a$ lattice, which clearly indicates that these two types of structure are different.

The values of the final agreement factor, Rwp, range between 4.0 and 5.5 % for the structures solved (Table 3), indicating a very good agreement between the calculated and experimental X-ray diffraction patterns. Besides, they do not differ markedly from the values obtained after Pawley refinement (Table 2), which did not take into account the

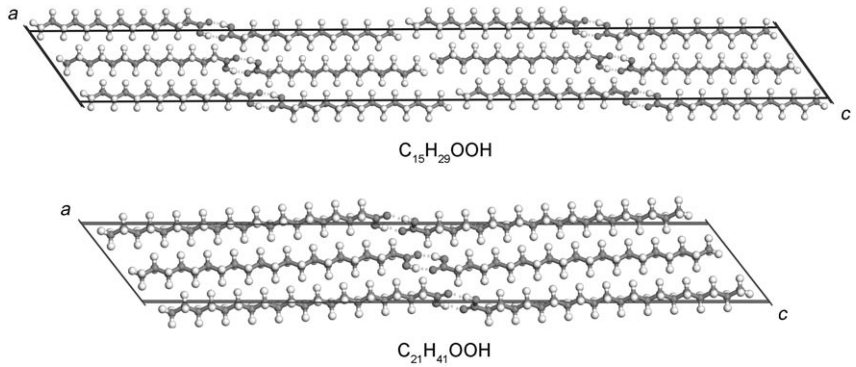

Figure 6. Representations in the (*a*,*c*) plane of the crystal structures of the high-temperature solid forms of $C_{15}H_{29}OOH$ (C″ form) and $C_{21}H_{41}OOH$ (C′ form).

Table 3. Selected structural data determined from the crystal structures of the C″ (this work and Bond's[6]) and C′ forms of the six fatty acids.

		Angle of tilt of the alkyl chain [°]		Packing arrangement of the carboxyl groups			H···H distances at the methyl-group interface [Å]			
	Rwp	towards *a* axis	towards *b* axis	C-C-C-O torsion angle [°]	O–H···O angle [°]	O···O distance [Å]	(0)–(1) and (0)–(2)		(0)–(3)	
$C_{13}H_{25}OOH$	0.041	125.8(3)	88.92(6)	3	165	2.54(4)	2.70	2.82	2.90	2.58
$C_{13}H_{25}OOH$[6]	–	–	–	179	177	2.63	–	–	–	2.51
$C_{15}H_{29}OOH$	0.047	125.2(2)	90.71(4)	4	164	2.55(4)	2.73	2.77	2.83	2.62
$C_{15}H_{29}OOH$[6]	–	–	–	179	156	2.63	–	–	–	2.60
$C_{17}H_{33}OOH$	0.054	125.2(3)	89.91(6)	7	161	2.72(9)	2.51	2.62	2.84	2.74
$C_{19}H_{37}OOH$	0.053	124.9(2)	89.49(5)	13	153	2.62(7)	2.49	2.69	3.01	2.92
$C_{21}H_{41}OOH$	0.055	124.6(1)	89.30(3)	9	152	2.60(5)	2.83	2.95	3.09	2.93
$C_{23}H_{45}OOH$	0.050	124.6(1)	89.62(4)	4	159	2.70(7)	2.74	2.80	2.84	3.07

agreement between the calculated and measured intensities of the various reflections. Table 3 also contains selected structural data that serve to describe the packing arrangement of the fatty acids within (alkyl chains, carboxyl groups) and between (methyl groups) the layers, and that have been determined from this work and from the C″ structures of $C_{13}H_{25}OOH$ and $C_{15}H_{29}OOH$ solved by Bond.

Description of the C″ structures and comparison with the single-crystal data:[6] The alkyl chains are packed in the orthorhombic packing arrangement O⊥, as described long ago by Bunn,[1] in accordance with the single-crystal structures. This motif is very common in long-chain aliphatic compounds.[4,5] The chains are almost parallel and the zigzag planes of neighbouring molecules are perpendicular to one another (Figure 7). Moreover, the alkyl chains are tilted from the (*a*,*b*) plane. The angles of tilt of the chain axis with respect to the *a* and *b* axes have been evaluated and are displayed in Table 3. The chains are almost perpendicular to the *b* axis, but are tilted towards the *a* axis with angles of 125.8° and 125.2° for $C_{13}H_{25}OOH$ and $C_{15}H_{29}OOH$, respectively. These values are consistent with those of the θ_1 angles (125.9° for $C_{13}H_{25}OOH$ and 125.3° for $C_{15}H_{29}OOH$), defined by Bond as the angle between the plane parallel to the chain axis and the methyl-group interface, in the present case the (*a*,*b*) plane.

A similar hydrogen-bonding framework is obtained for both the powder and single-crystal C″ structures of $C_{13}H_{25}OOH$ and $C_{15}H_{29}OOH$. The O–H···O angle formed between the acceptor and the donor in the hydrogen bond is close to 180° in both cases (Table 3), indicative of strong hydrogen bonds. The C-C-C-O torsion angle (O being the oxygen atom bearing the hydrogen atom) is close to 0° (this work) or 180° (Bond's work), which shows that the carboxyl group is always almost coplanar with the alkyl chain. However, there are discrepancies between the values obtained for the O···O distances, that is, around 2.63 Å in the single-crystal study (standard values for crystal structures of solid forms of fatty acids[23–26]) as opposed to much shorter distances in our study. The uncertainties in our values have been assessed by estimating the uncertainties in the positions of the oxygen atoms, as these were not available from the refinement program. Our measurements are much less precise (average deviation of 0.06 Å, taking into account the values obtained for the C′ structures) than those based on the single-crystal data (precision of around 0.01 Å). This lack of accuracy of the O···O distances is directly related to the method used for the crystal structure determination as the final structure is a compromise between the agreement of the measured and calculated X-ray powder-diffraction patterns and the energy minimisation. However, taking into account the evaluated uncertainties, the O···O distances de-

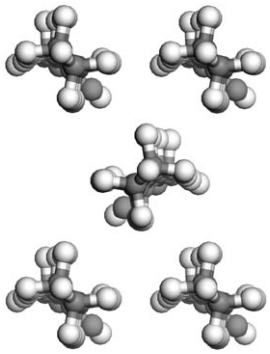

Figure 7. Packing arrangement of the alkyl chains of $C_{13}H_{25}OOH$ perpendicular to the chain axis.

termined from the powder data are almost consistent with those obtained from the single-crystal data.

At the methyl-group interface, the packing arrangement is also similar for the C″ structures determined by the two different techniques. A given methyl group, denoted as (0), just below the (*a*,*b*) plane has three closest neighbouring methyl groups just above the (*a*,*b*) plane, denoted as (1), (2), and (3) (see Figure 8). (1) and (2) are related to each other by a translation of the lattice along the *b* vector. They are situated either side of (0) along the *b* axis. (3) is situated almost immediately below (0) along the *a* axis. The shortest H···H distances between (0) and (3) are consistent between the two sets of data (Table 3).

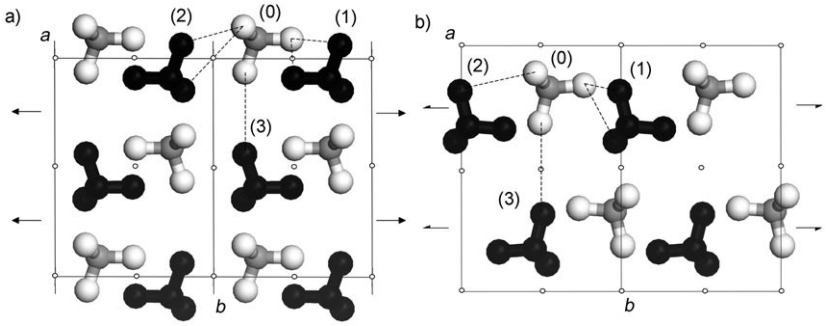

Figure 8. Packing arrangement of the methyl groups in the (*a*,*b*) plane at the methyl-group interface for a) $C_{15}H_{29}OOH$ and b) $C_{19}H_{37}OOH$. The methyl groups in black are just above the plane, the others are just below. The two arrangements are derived from one another by a translation of $^1/_2a+^1/_2b$ of one methyl-group layer with respect to the other.

Finally, it may be noted that the crystal structures of the C″ forms of $C_{13}H_{25}OOH$ and $C_{15}H_{29}OOH$ presented herein are in good agreement with those already solved from single-crystal data. Hence, it may be assumed that the crystal structures of the longer fatty acids determined by application of the same technique should be equally reliable.

Comparison of the C′ and C″ structures: The C′ and C″ forms exhibit a similar packing arrangement of the molecules within the bilayers. In the C′ structures, the alkyl chains are stacked in the orthorhombic packing arrangement O⊥, as in the case of the C″ structures. Moreover, they are tilted in the same way towards the (*a*,*b*) plane, at an angle close to 90° with respect to the *b* axis and at an angle of around 125° with respect to the *a* axis. As regards the packing arrangement of the carboxyl groups, no significant variation in the C-C-C-O torsion angle, the O–H···O angle, or the O···O distance can be seen on going from $C_{13}H_{25}OOH$ to $C_{23}H_{45}OOH$. In particular, the O···O distance ranges from 2.60 to 2.72 Å for the C′ structures, but taking into account the evaluated uncertainties, these values are all consistent with the 2.63 Å determined from the single-crystal C″ structures. One interesting point worthy of mention concerns the C-C-C-O torsion angle. For the six structures investigated, this parameter is close to 0° (it varies from 3 to 13°), which corresponds to a *trans* conformation of the carboxyl groups. On the other hand, the C-C-C-O torsion angle is close to 180° for the C″ structures solved by Bond, which corresponds to a *cis* conformation of the carboxyl groups. In the latter case, however, the C–O and C=O distances are very close (1.291(5) and 1.233(5) Å for $C_{13}H_{25}OOH$; 1.280(6) and 1.237(7) Å for $C_{15}H_{29}OOH$). Thus, it may well be the case that these structures exhibit both conformations, as Hayashi and Umemura have ascertained for several fatty acids from C_3H_5OOH to $C_{20}H_{39}OOH$ by means of polarized infrared spectroscopy.[27] In the present work, structures with a *cis* conformation of the carboxyl group, that is, with the C-C-C-O torsion angle equal to 180°, have also been tested. These structures were invariably found to be less energetically favourable than those featuring a *trans* conformation of the carboxyl groups. Although this result does not disprove that the actual structures might exhibit both conformations, it nevertheless indicates that the *trans* conformation must be the dominant one for the structures we have solved.

The crucial differences between the C′ and C″ structures lie in the packing arrangements at the methyl-group interface. Figure 8 shows the packing arrangements of the methyl groups in the (*a*,*b*) plane for the C″ form of $C_{15}H_{29}OOH$ and the C′ form of $C_{19}H_{37}OOH$. The methyl groups of the molecules above the plane are shaded black, whereas those situated just below the plane are in grey. (0) has three closest neighbours above the methyl-group interface, (1), (2) and (3), which are situated at similar positions relative to (0) in both the C′ and C″ structures. However, (1), (2) and (3) are differently related to (0) in terms of the symmetry elements involved, and hence according to the space groups. In the *A*2/*a* structures (C″ form), (1) and (2) are related to (0) through inversion centres, whereas they are related by a 2_1 axis in the $P2_1/a$ structures (C′ form). Thus, (1) and (2) are equidistant from (0) in the $P2_1/a$ structures, whereas in the *A*2/*a* structures the relative positions of (1) and (2) with respect to (0) depend on the relative position of (0) with respect to the inversion centres. (3) is related to (0) by a 2 axis in the *A*2/*a* structures, whereas it is related by an inversion centre in the $P2_1/a$ structures. The shortest H···H distances measured between (0) and its three closest neighbours exceed 2.4 Å (sum of the van der Waals radii of two hydrogen atoms) in each of the six structures (Table 3). It may also be noted that the distances between the hydrogen atoms of (0) and (3) increase with increasing chain length. This trend can be attributed to the increased thermal motion, as the temperature of measurement also increases with increasing chain length. Actually, the C′ and C″ forms contain identical 2D layers: the methyl group ar-

rangements in both the above and below layers (in black and grey, respectively, in Figure 8) are the same for the $P2_1/a$ and $A2/a$ structures. The difference between these structures lies in the way in which these layers are stacked. It can clearly be seen in Figure 8 that when (1), (2) and (3) are displaced along the $1/2a+1/2b$ vector in the $P2_1/a$ structure (or $A2/a$ structure), they become related to (0) with the symmetry elements involved in the $A2/a$ arrangement (or $P2_1/a$ arrangement).

Discussion

According to the crystal structures of the high-temperature phases of odd-numbered fatty acids determined in the present work and in that of Bond,[6] the C′′ form is only seen for $C_{13}H_{25}OOH$ and $C_{15}H_{33}OOH$ in the series from $C_7H_{13}OOH$ to $C_{23}H_{45}OOH$. The question then arises as to why this solid phase is only adopted by these two fatty acids. In the following, we propose an explanation based on a survey of the energetic contributions that are operative in the packing arrangements of the molecules within the C′ and C′′ crystal structures.

Two major intermolecular interactions are involved in the cohesion of the structures of the high-temperature phases of fatty acids, namely hydrogen bonds and van der Waals interactions. The former influence the packing arrangement of the carboxyl groups, whereas the latter relate more to the interactions between the atoms of the hydrocarbon chains. These two interactions are evaluated in the potential-energy descriptions of the structures through van der Waals and electrostatic contributions. The overall potential energies of the structures and the potential energies of the latter two contributions are listed in Table 4 for the six structures investigated, together with those determined from the crystal structures of the high-temperature phases of the odd-numbered fatty acids solved by Bond (from $C_7H_{13}OOH$ to $C_{15}H_{29}OOH$). The energy values are given in kJ mol^{-1} per molecule, so that they can be compared for all of the structures.

Table 4. Potential energies (per molecule) calculated from the crystal structures of the high-temperature solid forms of odd-numbered fatty acids solved in this work and in that of Bond.[6]

	Total energy [kJ mol^{-1}]	Intermolecuar interactions Electrostatic [kJ mol^{-1}]	van der Waals [kJ mol^{-1}]
reference [6]			
$C_7H_{13}OOH$	−278(4)	−158	−52
$C_9H_{17}OOH$	−316(4)	−159	−64
$C_{11}H_{21}OOH$	−354(4)	−159	−75
$C_{13}H_{25}OOH$	−394(4)	−158	−90
$C_{15}H_{29}OOH$	−436(4)	−158	−105
this work			
$C_{13}H_{25}OOH$	−392(2)	−165	−73
$C_{15}H_{29}OOH$	−432(2)	−165	−88
$C_{17}H_{33}OOH$	−472(2)	−158	−113
$C_{19}H_{37}OOH$	−511(4)	−160	−122
$C_{21}H_{41}OOH$	−551(3)	−161	−132
$C_{23}H_{45}OOH$	−596(2)	−158	−154

The electrostatic potential energy is practically constant for all of the structures (around −160 kJ mol^{-1}), whether determined from the powder or single-crystal data. This is consistent with the similar packing of the carboxyl groups within the dimers established for the six structures investigated. However, the values obtained for the C′′ structures do differ a little between our work and that of Bond. This may be related to the discrepancy between the O···O distances mentioned in the previous section (2.54 and 2.55 Å for our structures, as compared to 2.63 Å for Bond's structures). The potential energy of the hydrogen bonds is higher than the van der Waals potential energy for each structure. This confirms the predominant role of the hydrogen bonds in the cohesion of these crystal structures. However, the van der Waals forces increase with increasing chain length, and in the case of $C_{23}H_{45}OOH$ the potential energies of the two interactions are almost equal. The evolution of the total energy of the structures of the high-temperature phases with increasing chain length produces a straight line from $C_7H_{13}OOH$ to $C_{23}H_{45}OOH$ (Figure 9), irrespective of the solid phase considered. This linear trend confirms the similarity of the molecular arrangements in the C′ and C′′ phases. It also implies that the energy barrier between the two solid forms must be very low.

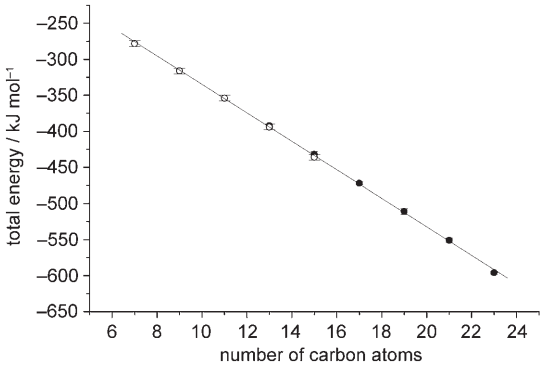

Figure 9. Evolution of the total energy of the high-temperature structures of the odd-numbered fatty acids with chain length from $C_7H_{13}OOH$ to $C_{23}H_{45}OOH$. ●: the structures determined by us; ○: the structures solved by Bond.[6]

A third contribution, which has already been invoked several times in this paper, also exerts an influence on the packing arrangement of the molecules, namely that of thermal motion. Indeed, the high-temperature phases are only stable in a narrow temperature range below the melting points, this range narrowing with increasing chain length, as the temperatures of transition to C′ or C′′ and of melting increase. Thus, the effect of thermal motion has to be studied if we want to thoroughly understand the packing arrangement of the molecules in these particular solid forms.

When considering the equivalent temperature factors, U_{eq}, of the non-hydrogen atoms of the odd-numbered fatty acids

from $C_7H_{13}OOH$ to $C_{15}H_{29}OOH$ determined from the single-crystal data,[6] it appears that thermal agitation exerts a greater effect on the last few carbon atoms of the chains, that is, on those close to the terminal methyl group for each compound. These temperature factors are represented in Figure 10 for the non-hydrogen atoms of these five acids.

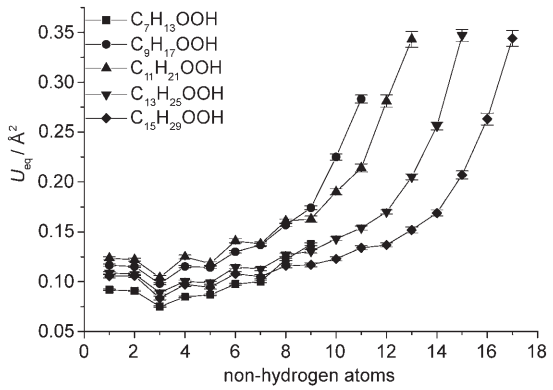

Figure 10. Evolution along the hydrocarbon chains of the equivalent temperature factors (U_{eq}) determined by Bond for the non-hydrogen atoms of the odd-numbered fatty acids from $C_7H_{13}OOH$ to $C_{15}H_{29}OOH$. 1 and 2 correspond to the two oxygen atoms; 3 to n+2 (where n is the total number of carbon atoms) denote the carbon atoms from the carboxyl group to the methyl group. The temperature factors have been linked for each molecule.

The atoms are labelled from 1 to n+2 (in which n is the total number of carbon atoms), 1 and 2 denoting the two oxygen atoms and the integers from 3 to n+2 denoting the carbon atoms of the hydrocarbon chains from the carboxyl group to the methyl group. It can be seen from this representation that, for the five acids, the temperature factors are much higher for the atoms near the methyl group than for the others. It can be assumed that the strong hydrogen bonds counteract the thermal agitation and limit the motion of the atoms near the carboxyl group. Thus, for a given molecule, the further the atoms are from the carboxyl group, the weaker the effect of the hydrogen bonds and the more prone they will be to the effect of thermal agitation. This trend is clearly apparent in Figure 10.

As the structures of the fatty acids from $C_{17}H_{33}OOH$ to $C_{23}H_{45}OOH$ were solved by assuming the molecules to be rigid bodies, a global isotropic temperature factor was determined for each structure, which accounts for the mean thermal agitation within the structure. Our aim was to investigate the evolution of the thermal agitation for the high-temperature solid forms of the odd-numbered fatty acids from $C_7H_{13}OOH$ to $C_{23}H_{45}OOH$. For $C_7H_{13}OOH$, $C_9H_{17}OOH$, and $C_{11}H_{21}OOH$, we summed the values of the equivalent temperature factors of the non-hydrogen atoms and divided the result by the number of atoms considered. Thereby, we obtained mean temperature factors that could be compared with the global isotropic factors determined for the six longer fatty acids. All of these temperature factors are gathered in Table 5. In addition, the temperature at which the measurement was undertaken as well as the melting point are also indicated in each case.

Table 5. Mean temperature (T) factors determined for the high-temperature phases of the odd-numbered fatty acids from $C_7H_{13}OOH$ to $C_{23}H_{45}OOH$.

	T_{meas} [K]	$T_{melting}$ [K]	Ref.	Mean T factor [Å^2]
$C_7H_{13}OOH$	230.0	265.83(1)	[12]	0.099(1)
$C_9H_{17}OOH$	270.0	285.53(1)	[12]	0.151(2)
$C_{11}H_{21}OOH$	300.0	301.63(1)	[12]	0.171(3)
$C_{13}H_{25}OOH$	313.0	314.6(5)	this work	0.217(6)
$C_{15}H_{29}OOH$	324.0	325.5(4)	this work	0.191(5)
$C_{17}H_{33}OOH$	333.0	333.5(5)	this work	0.174(6)
$C_{19}H_{37}OOH$	340.0	340.4(3)	this work	0.099(5)
$C_{21}H_{41}OOH$	346.4	346.7(5)	this work	0.063(4)
$C_{23}H_{45}OOH$	351.7	352.0(5)	this work	0.073(4)

It is noteworthy that the values obtained for the mean temperature factors are not very accurate because they can be affected by systematic errors in the measured intensities. Moreover, the X-ray diffraction measurements were performed close to the melting points (within about 1 K) for all of the acids except $C_7H_{13}OOH$ and $C_9H_{17}OOH$ (around 35 and 15 K below their melting points, respectively), which introduces further uncertainty in the values. However, we are more interested here in the evolution of these values across the series than in the values themselves. Considering that the measurements were made under approximately the same conditions for all of the fatty acids, it can be assumed that all of the temperature factors can be compared. Their evolution in relation to the chain length is plotted in Figure 11. It appears that they increase up to $C_{13}H_{25}OOH$ and then decrease once more.

The particular evolution obtained may be explained in terms of the competitive effects of van der Waals forces and thermal agitation, both of which increase with increasing chain length, whereas the hydrogen bonds remain approximately constant for all of the structures. The ascending part of the curve may be related to a predominance of the effect

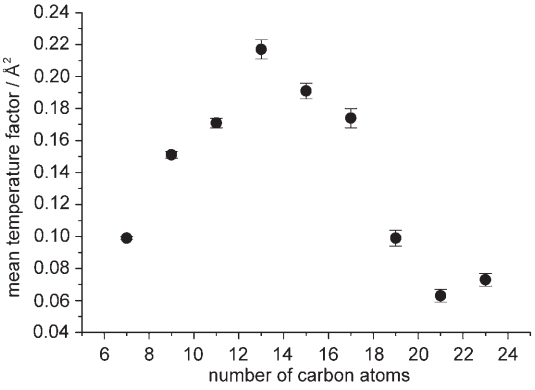

Figure 11. Evolution of the mean temperature factors determined for the high-temperature phases of the odd-numbered fatty acids with chain length from $C_7H_{13}OOH$ to $C_{23}H_{45}OOH$. The values have been calculated from the data of Bond for the fatty acids from $C_7H_{13}OOH$ to $C_{11}H_{21}OOH$, and come from our own results for the longer acids.

of thermal agitation, whereas for the descending part the van der Waals forces should prevail. In this representation, it is also apparent that the displacements due to temperature are, on average, more significant for $C_{13}H_{25}OOH$ and $C_{15}H_{29}OOH$. As can be seen in Figure 10, the greatest displacements are certainly located near the methyl group. Moreover, according to van de Streek et al.,[28] who studied the influence of thermal motion on the crystal structures of *n*-alkanes, they should be mostly oriented perpendicular to the chain axis, approximately in the (*a*,*b*) plane in our case. Keeping in mind that the C′ and C″ arrangements are mutually related by a translation of a layer in the (*a*,*b*) plane and also that the energy barrier between the two solid forms is certainly very low, notably in the cases of $C_{13}H_{25}OOH$ and $C_{15}H_{29}OOH$, the competitive effects of van der Waals forces and thermal motion are more conducive to adoption of the C″ form. A similar conclusion was reached by van de Streek and co-workers concerning the relative stabilities of the triclinic and monoclinic polymorphs of even-numbered *n*-alkanes with increasing chain length. For the other acids, we surmise that the effect of thermal agitation is not strong enough since, on the one hand, for the shorter acids the transition temperatures are not very high (and consequently nor is the thermal motion), while, on the other hand, the van der Waals forces become stronger for the longer acids. This may explain why, as far as we are aware, the C″ form is only adopted by $C_{13}H_{25}OOH$ and $C_{15}H_{29}OOH$.

Conclusion

The crystal structures of the high-temperature solid forms of the odd-numbered fatty acids from $C_{13}H_{25}OOH$ to $C_{23}H_{45}OOH$ have been determined from X-ray powder-diffraction patterns. $C_{13}H_{25}OOH$ and $C_{15}H_{29}OOH$ have been found to adopt the C″ form at high temperatures, as also shown by Bond.[6] However, we have proved that the C′ form is adopted by the longer fatty acids, as is also the case for the shorter fatty acids from $C_7H_{13}OOH$ to $C_{11}H_{21}OOH$ according to Bond.[6] Thus, C″ is only observed for $C_{13}H_{25}OOH$ and $C_{15}H_{29}OOH$. The C″ and C′ forms are both monoclinic, but the former has the space group $A2/a$ with $Z=8$, whereas the latter has the space group $P2_1/a$ with $Z=4$. Both of their structures consist of bilayers of molecules held together by hydrogen bonds between their carboxyl groups. The packing arrangement in the two types of structures is very similar. The major differences lie at the methyl-group interface. It has been shown that the packing arrangements of the molecules in these high-temperature solid forms of odd-numbered fatty acids are determined by the balance of the competitive effects due, on the one hand, to hydrogen bonds and van der Waals interactions, which serve to hold the structure together, and, on the other hand, thermal motion, which tends to push the molecules apart.

Lastly, this article proves the validity of the technique that we have used to solve crystal structures from X-ray powder-diffraction data, as the results obtained for the C″ forms of $C_{13}H_{25}OOH$ and $C_{15}H_{29}OOH$ compare well with those obtained from single crystals. However, some improvements have to be made regarding the assessment of the hydrogen bonds, considering in particular the low precision of the O···O distances.

Experimental Section

Materials: Highly pure samples of $C_{13}H_{25}OOH$, $C_{15}H_{29}OOH$, $C_{17}H_{33}OOH$, $C_{19}H_{37}OOH$, $C_{21}H_{41}OOH$, and $C_{23}H_{45}OOH$ were supplied by Fluka. The purities of all these compounds are estimated by the supplier to exceed 99%.

Thermal analysis: Transition temperatures as well as enthalpy changes were determined by using a Perkin–Elmer DSC-7 instrument equipped with a cooling accessory, which allowed the temperature to be increased from 110 to 950 K. A heating rate of 2 K min^{-1} was typically used. Measurements at lower heating rates (0.5, 0.2 K min^{-1}) were also performed in order to better resolve transitions occurring at close temperatures. Samples (about 4 mg) were placed in aluminium pans and weighed before and after each experiment in order to determine the mass loss. At least six measurements were performed on each compound to enable the calculation of accurate values of the various thermodynamic quantities. The uncertainties in the temperatures and enthalpies were determined by using Student's method[29] with a 95% threshold of reliability. To this value was added the systematic error arising from the calibration of the apparatus, which was set at ± 0.2 K for the temperatures and ± 1% for the enthalpies.

X-ray powder diffraction: An Inel CPS 120 X-ray powder diffractometer was used to obtain high-quality powder-diffraction patterns of the high-temperature solid forms. $Cu_{K\alpha}$ radiation was selected for the incident beam. The diffractometer was equipped with an Oxford Cryosystems N_2 cryostream to facilitate the performance of isothermal experiments at different selected temperatures. The Inel CPS 120 diffractometer operates with Debye–Scherrer transmission geometry and the diffracted beams are collected on a 120° curved counter by gas ionisation (argon + C_2H_6). The sample is introduced in a 0.5 mm diameter Lindemann glass capillary. The latter is rotated about its axis during the experiment in order to minimise preferential orientations of the crystallites. The acquisition time was set at six hours in order to obtain reflections with exploitable intensities. The relative heights of the strongest reflections at the start of each measurement were compared with those obtained for the X-ray powder-diffraction pattern of the B′ form of $C_{17}H_{33}OOH$, which was calculated from the structure published by Goto and Asada[23] based on a study carried out on single crystals. Then, we chose the samples for which the agreement was best, assuming that the intensities in the calculated X-ray powder-diffraction pattern of the B′ form of $C_{17}H_{33}OOH$ were free from any preferential orientation effect. As recommended,[30] external calibration to convert the measured 4096 channels to 2θ degrees was applied by means of cubic spline fittings using cubic $Na_2Ca_2Al_2F_4$. The latter was combined with a low-angle calibration using silver behenate,[31] a material that exhibits several reflections in the 2θ range of 1.5–20°.

Determination of cell parameters and space groups: The peak positions were determined after pseudo-Voigt fitting using DIFFRACTINEL software. Potential solutions of cell parameters and space groups were obtained using X-CELL software[32] available in the module POWDER INDEXING of MATERIAL STUDIO. The cell parameters and space group that best corresponded to the experimental X-ray diffraction pattern of the solid form under investigation were finally determined using a Pawley profile-fitting procedure.[21] The latter provided the refinement of the cell parameters, the peak profile parameters (function of profile, FWHM, asymmetry), the background, and the zero shift.

Determination of the crystal structures: The molecule to be studied was drawn in a 3D worksheet and was minimised in energy by means of geometry optimisation using the COMPASS force field[33] to obtain the relevant distances, angles, and dihedral angles for its various bonds. This

molecule was then set as a rigid body, but with the dihedral angle of the carboxyl group allowed to adjust freely, as this determines the good establishment of the hydrogen bonds. The rigid body was introduced in the cell whose dimensions had been previously found, together with its homologues related to the space group. The whole system was moved in the cell according to the seven degrees of freedom (three translations, three rotations, and the dihedral angle of the carboxyl group) by using a Monte Carlo-type simulation[18] over several cycles to obtain the best reproduction of the experimental X-ray powder-diffraction pattern by the calculated one. The final structure was then obtained after repeated alternating application of Rietveld refinement[34] and geometry optimisation by energy minimisation in order to reach the best agreement between X-ray powder diffraction and molecular interactions. The Rietveld procedure includes refinement of the translations, rotations, and dihedral angle of the molecule, the isotropic temperature factors, and the preferred orientations, also with the parameters previously refined in the Pawley procedure. The total energy determined for the structures corresponds to a survey of the intra- and intermolecular interactions involved. Its entire expression is given in an article by Sun.[33]

CCDC-612518 to CCDC-612523 contain the supplementary crystallographic data for this paper. These data can be obtained free of charge via www.ccdc.cam.ac.uk/data_request/cif.

[1] C. W. Bunn, *Trans. Faraday Soc.* **1939**, *35*, 482–491.
[2] E. von Sydow, *Ark. Kemi* **1955**, *9*, 231–254.
[3] S. Abrahamsson, B. Dahlen, H. Löfgren, I. Pascher, *Prog. Chem. Fats Other Lipids* **1978**, *16*, 125–143.
[4] L. Hernqvist, in *Crystallization and Polymorphism of Fats and Fatty Acids* (Eds.: N. Garti, K. Sato), Marcel Dekker, New York, **1988**, pp. 97–137.
[5] J. Yano, K. Sato, *Food Res. Int.* **1999**, *32*, 249–259.
[6] A. D. Bond, *New J. Chem.* **2004**, *28*, 104–114.
[7] F. Francis, S. H. Piper, T. Malkin, *Proc. R. Soc London, Ser. A* **1930**, *128*, 214–252.
[8] M. Kobayashi, F. Kaneko, *J. Dispersion Sci. Technol.* **1989**, *10*, 319–350.
[9] M. Gotoh, *J. Jpn. Oil Chem. Soc.* **1987**, *36*, 12, 909–919.
[10] E. Moreno, R. Cordobilla, T. Calvet, M. A. Cuevas-Diarte, G. Gbabode, P. Negrier, D. Mondieig, H. A. J. Oonk, unpublished results.
[11] E. von Sydow, *Acta Crystallogr.* **1955**, *8*, 810–813.
[12] F. Rajabalee, V. Metivaud, H. A. J. Oonk, D. Mondieig, P. Waldner, *Phys. Chem. Chem. Phys.* **2000**, *2*, 1345–1350.
[13] H. A. J. Oonk, D. Mondieig, Y. Haget, M. A. Cuevas-Diarte, *J. Chem. Phys.* **1998**, *108(2)*, 715–722.
[14] L. Ventolà, T. Calvet, M. A. Cuevas-Diarte, D. Mondieig, H. A. J. Oonk, *Phys. Chem. Chem. Phys.* **2002**, *4*, 1953–1956.
[15] L. Ventolà, T. Calvet, M. A. Cuevas-Diarte, X. Solans, D. Mondieig, P. Negrier, J. C. van Miltenburg, *Phys. Chem. Chem. Phys.* **2003**, *5*, 947–952.
[16] E. Stenhagen, E. von Sydow, *Ark. Kemi* **1953**, *6*, 309–316.
[17] R. C. F. Schaake, J. C. van Miltenburg, C. G. de Kruif, *J. Chem. Thermodyn.* **1982**, *14*, 763–769.
[18] G. E. Engel, S. Wilke, O. König, K. D. M. Harris, F. J. J. Leusen, *J. Appl. Crystallogr.* **1999**, *32*, 1169–1179.
[19] MS Modeling (Material Studio) version 3.0: http://www.accelrys.com/mstudio/ms_modeling.
[20] F. Kaneko, J. Yano, H. Tsujiuchi, K. Tashiro, M. Suzuki, *J. Phys. Chem. B* **1998**, *102(2)*, 6184–6187.
[21] G. S. Pawley, *J. Appl. Crystallogr.* **1981**, *14*, 357–361.
[22] http://fazil.rajabalee.free.fr/delphi_an.htm
[23] M. Goto, E. Asada, *Bull. Chem. Soc. Jpn.* **1984**, *57*, 1145–1146.
[24] G. Gbabode, P. Negrier, D. Mondieig, J. M. Leger, T. Calvet, M. A. Cuevas-Diarte, *Anal. Sci.* 2006, 22, x269–x270.
[25] F. Kaneko, M. Sakashita, M. Kobayashi, Y. Kitagawa, Y. Matsuura, M. Suzuki, *Acta Crystallogr. Sect. C* **1994**, *C50*, 245–247.
[26] F. Kaneko, M. Sakashita, M. Kobayashi, Y. Kitagawa, Y. Matsuura, M. Suzuki, *Acta Crystallogr. Sect. C* **1994**, *C50*, 247–250.
[27] S. Hayashi, J. Umemura, *J. Chem. Phys.* **1975**, *63*, 5, 1732–1740.
[28] J. van de Streek, P. Verwer, P. Bennema, E. Vlieg, *Acta Crystallogr. Sect. B* **2002**, *B58*, 677–683.
[29] Y. V. Linnink, *La Méthode des Moindres Carrés* (translated into French by O. Arkhipoff), Dunod, Paris, **1963**.
[30] M. Evain, P. Deniard, A. Jouanneaux, R. Brec, *J. Appl. Crystallogr.* **1993**, *26*, 563–569.
[31] T. C. Huang, H. Toraya, T. N. Blanton, Y. Wu, *J. Appl. Crystallogr.* **1993**, *26*, 180–184.
[32] M. A. Neumann, *J. Appl. Crystallogr.* **2003**, *36*, 356–365.
[33] H. Sun, *J. Phys. Chem. B* **1998**, *102*, 7338–7364.
[34] H. M. Rietveld, *J. Appl. Crystallogr.* **1969**, *2*, 65–71.

Received: July 4, 2006
Revised: October 25, 2006
Published online: January 10, 2007

